Informes Técnicos Ciemat

1022

Septiembre, 2003

Feasibility Study on a Neutral Beam Diagnostic Injector for TJ-II

K. J. McCarthy
R. Balbín
A. López-Fraguas

Asociación EURATOM/CIEMAT para Fusión - 86

Departamento de Fusión y Física de Partículas Elementales

Toda correspondenica en relación con este trabajo debe dirigirse al Servicio de Información y Documentación, Centro de Investigaciones Energéticas, Medioambientales y Tecnológicas, Ciudad Universitaria, 28040-MADRID, ESPAÑA.

Las solicitudes de ejemplares deben dirigirse a este mismo Servicio.

Los descriptores se han seleccionado del Thesauro del DOE para describir las materias que contiene este informe con vistas a su recuperación. La catalogación se ha hecho utilizando el documento DOE/TIC-4602 (Rev. 1) Descriptive Cataloguing On-Line, y la clasificación de acuerdo con el documento DOE/TIC.4584-R7 Subject Categories and Scope publicados por el Office of Scientific and Technical Information del Departamento de Energía de los Estdos Unidos.

Depósito Legal: M -14226-1995
ISSN: 1135 - 9420
NIPO: 402-03-005-6

Editorial CIEMAT

CLASIFICACIÓN DOE Y DESCRIPTORES

S70
NEUTRAL ATOM BEAM INJECTION; CHARGE EXCHANGE; NEUTRAL PARTICLE ANALYZERS; STELLARATORS; SPECTROSCOPY; PLASMA DIAGNOSTICS; MAGNETIC CONFINEMENT; TOKAMAK DEVICES

Feasibility Study on a Neutral Beam Diagnostic Injector for TJ-II

McCarthy, K.J.; Balbín, R.; López-Fraguas, A.
36 pp. 10 figs. 6 tbls. 31 refs.

Abstract

A diagnostic neutral beam system is proposed for the TJ-II stellarator. The main goal of installing such a system in TJ-II is to increase the signal to noise ratio and provide spatial resolution in diagnostic systems based on Charge Exchange Recombination Spectroscopy and Neutral Partióle Analysis, while also opening up new opportunities for physics studies in this magnetically confined plasma device. After outlining the unique characteristics of the TJ-II and reviewing available diagnostic injector systems, the compact system selected for TJ-II is presented together with estímales of the resulting increased signal levéis Finally other important aspects are discussed, in particular its location and orientation, as well as possible solutions to avoid perturbating the TJ-II magnetic configurations in the heliac device.

Estudio de la Viabilidad de un Inyector de Haz Neutro para Diagnosticar el TJ-II

McCarthy, K.J.; Balbín, R.; López-Fraguas, A.
36 pp. 10 figs. 6 tbls. 31 refs.

Resumen

Se propone desarrollar un sistema de inyección de haces de neutros para diagnóstico en el stellarator TJ-II. El principal objetivo de este tipo de sistema en el TJ-II es incrementar la razón señal-ruido y proporcionar resolución espacial en sistemas de diagnóstico que se fundamentan en la espectroscopia de recombinación por intercambio de carga y el análisis de energías de partículas neutras. Proporcionará también nuevas oportunidades para los estudios de física de este dispositivo de confinamiento magnético. Después de señalar las características exclusivas del TJ-II y estudiar los sistemas de inyección de diagnóstico disponibles, se presenta el sistema compacto seleccionado para TJ-II junto con las estimaciones realizadas de las mejoras de señal que resultarán de la aplicación de este sistema. Finalmente se discuten otros aspectos importantes, en particular la localización y orientación del haz, así como posibles soluciones para evitar la perturbación del sistema sobre las configuraciones magnéticas del TJ-II.

INDEX

I. Introduction

Neutral beam injectors have been used for several decades to study magnetically confined plasmas. Indeed, dedicated low divergence, quasi-stationary neutral beams, normally called Diagnostic Injectors (DI), are now common in most middle and large-scale plasma devices. Such systems permit localised information to be obtained on some basic plasma parameters by increasing the neutral density at the plasma centre and hence increasing the signal to noise ratio and spatial resolution in systems such as Charge Exchange (CX) Neutral Particle Analysers (NPA) or spectrometers. These parameters include the majority and impurity ion temperatures as well as plasma velocity. In addition, DI beams are used in many machines for the measurement of the majority ion equilibrium and fluctuating velocity and temperature by Rutherford scattering (RS), for measurement of the impurity ion velocity and temperature by charge exchange recombination spectroscopy (CXRS), for magnetic field measurements via motional Stark effect (MSE) and for measurement of CX neutrals energy distribution functions by neutral particle analysers that will provide the ion temperature. It is now intended to develop a DI system for the TJ-II stellarator in order to further increase the scientific return of the four-period heliac device.

The most important requirements for such beams are sufficient current and high particle energy, so that the beam can penetrate to the plasma core. Also the beam duration should be sufficiently long to achieve good signal to noise ratios in the supporting diagnostics, while the beam should be well focussed in order to allow localised measurements to be made. In recent years, a concentrated effort has been made to develop systems for large fusion devices with extreme plasma conditions and long pulses. One such example is the Russian Diagnostic Injector (RUDI) system developed in Julich, Germany, in a joint collaboration between the Institut fur Plasmaphysik at Julich and the Budker Institute of Nuclear Physics at Novosibirsk, Russia [1].

In the following sections, new and innovative physical studies that could be made in the TJ-II by the provision of a DI are outlined. Then, several standard DI system types are described briefly and their suitability for the TJ-II stellarator is assessed with regard to neutral particle analysis and charge-exchange recombination spectroscopy techniques. Finally, other important considerations are also addressed, such as ion source shielding and beam orientation.

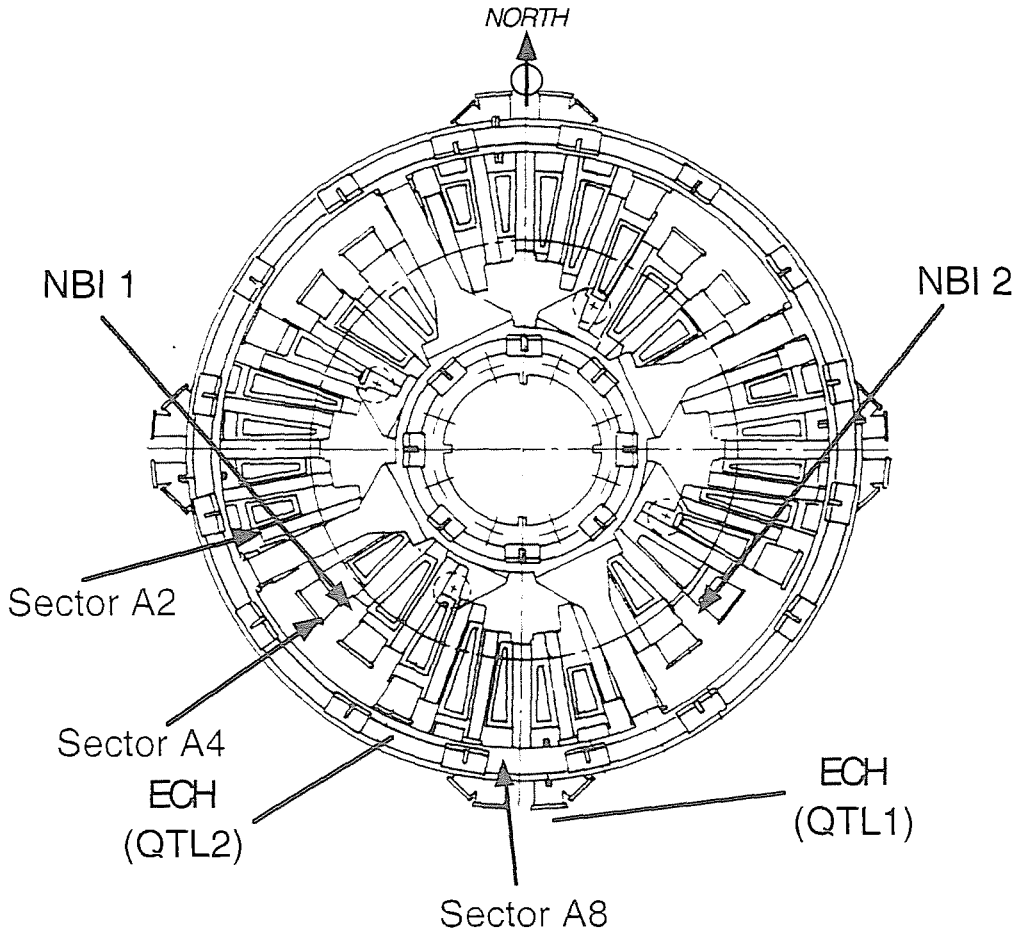

Figure 1. Layout of the TJ-II stellarator (as seen from above). The Neutral Beam Injection ports and trajectories (NBI 1 & 2) and the microwave injection ports (QTL1 and QTL2) are indicated. Sector A8 has been reserved for the Diagnostic Injector. Note that NBI 1 injection is parallel to the magnetic field (*i.e.* counter injection).

II. TJ-II characteristics and Diagnostic Injector requirements

i) *TJ-II description*

The TJ-II is a low magnetic shear stellarator of the heliac type with an average major radius of 1.5 m and an average minor radius of ≤ 0.22 m [2]. The size and shape of the plasma depends on the magnetic configuration, but in general the plasma cross-section can be considered as bean shaped [3]. Also its central magnetic field strength is about 1 T. It is operated with two gyrotrons working at 53.2 GHz (QTL1 & QTL2) that deliver up to 600 kW of electron cyclotron resonance heating (ECRH) to the plasma in X-mode. See Fig. 1. Under such conditions central electron densities can range from 0.5 to 1.2×10^{19} m^{-3}, the central electron temperature extends from 0.5 to 2 keV, while the central ion temperature (proton) ranges from 90 to 120 eV. In the near future up to 2 MW of additional heating will be

provided by two Neutral Beam Injectors (NBI) currently being commissioned [4]. With this additional heating, it is expected that the central electron density will be $\leq 10^{20}$ m^{-3}. This is an important point for consideration, as the diagnostic beam penetration is very dependent on electron density. For instance, the W7-AS diagnostic beam cannot be operated when electron densities are greater than ~10^{20} m^{-3} [5].

ii) *DI location*

The location of the DI in the TJ-II, which a four-period device with a complicated geometry, is an important point for consideration. However, the choice of locations is limited due to considerations such as occupancy [6], NBI shadow, orientation of the magnetic configuration about the central axis, and the space available. In the discussions that follow, we consider that the DI will be located in sector A8 with the DI ion source and neutraliser positioned either above the TJ-II or on the outer side of TJ-II, see Fig. 2. Note, that at this location, although not appreciable from Fig. 1, the DI is in the shadow of both NBI heating beams. Now in the first case, the neutral beam traverses the plasma vertically downwards (the beam is considered to be a neutral hydrogen beam) with the main diagnostic elements, a neutral particle analyser (NPA) [7] and a multi-channel fibre based spectrometer system, viewing the diagnostic beam from the A8 side-port. Note that the plasma cannot be viewed from the inner side of the TJ-II. In the second case, the neutral beam traverses the plasma at an acute angle to the horizontal from the A8 side-port towards the TJ-II hardcore. In this case, because of the difficulties foreseen to mount it vertically, the NPA views the beam from the side-port while the multi-channel fibres are positioned in the A8 upper and lower ports. However, in order to provide sufficient space for the DI it would be necessary to remove the current Acord-12 analyser from the current NPA system set-up [7]. In Section VII, the benefits and difficulties, from both technical and physics points of view, of both positions are discussed in more details.

Finally, as the TJ-II is a stellarator device, whose magnetic configurations are created by toroidal and poloidal magnetic coils, the perturbation effect of the magnetic shielding surrounding the ion source on the configuration is a primary factor when defining the ion source accelerating grid to plasma centre distance. On the other-hand, the ion source location, (above, below or to the side of the TJ-II), is only of secondary importance for such perturbations. These points are also discussed in Section VI.

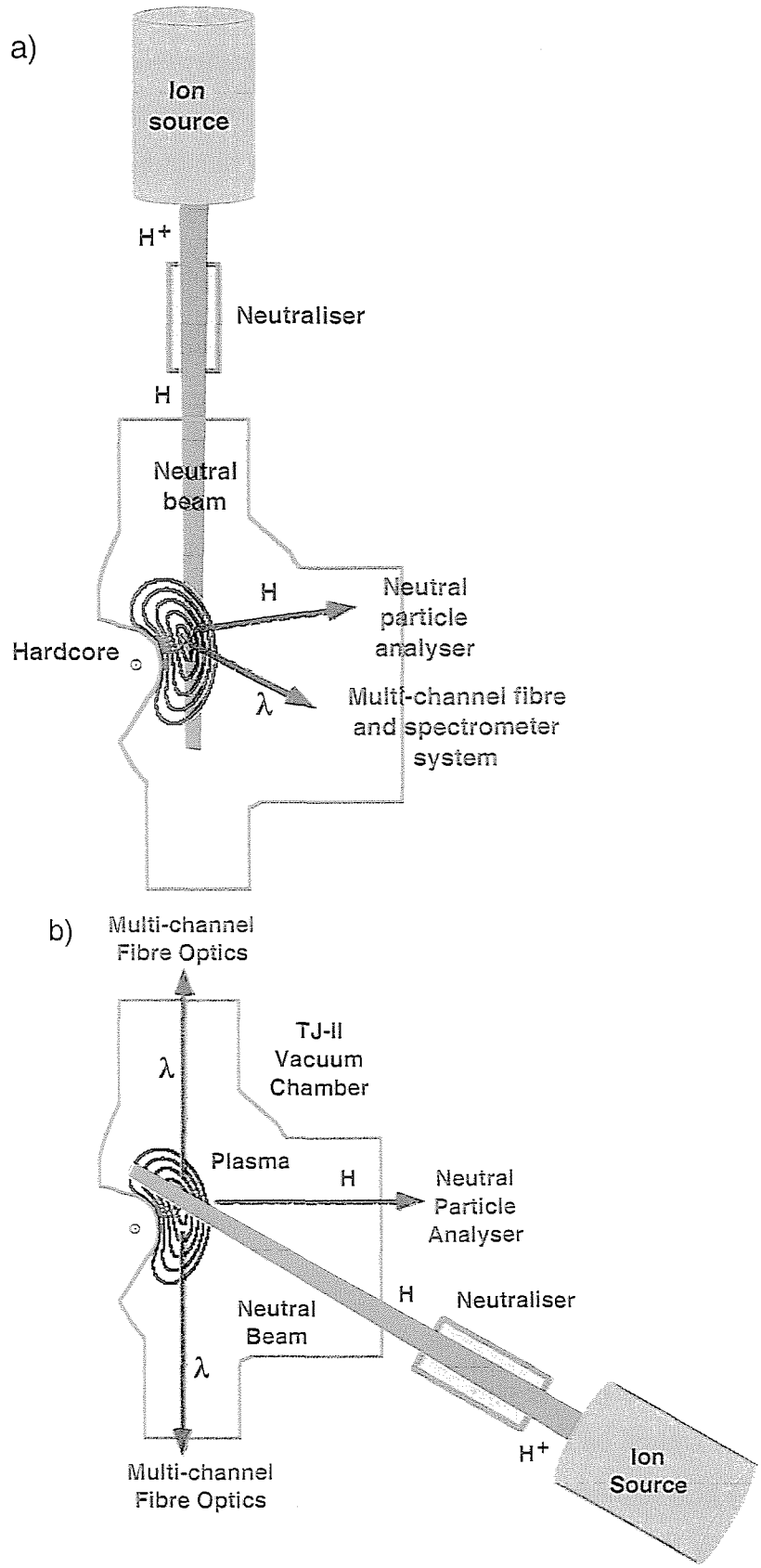

Figure 2. Cross-section through sector A8 in which the DI and its neutraliser box are located a) above and b) to the side of the TJ-II. For each case the relative positions of the principal diagnostics are also indicated.

III. Opportunities for Physics in the TJ-II

The provision of a DI in TJ-II will allow basic parameters such as the majority ion and impurity ion temperatures, and the plasma velocity to be determined with spatial resolution using standard techniques, *i.e.* neutral particle analysis and charge exchange recombination spectroscopy (CXRS). In addition, the provision of DI neutral beams in other magnetically confined plasma devices has opened the way for several study areas. For instance, the Motional Stark effect (MSE) has been used to measure local plasma magnetic and electric fields and the q-profile [8, 9] while Beam Emission Spectroscopy (BES) has been employed to determine local plasma densities and to study local density fluctuations [10-12]. Furthermore, CXRS yields central impurity densities (an absolutely calibrated spectrometer is needed) and temperatures as well as localised plasma flow velocities [13,14], while Rutherford Scattering (RS) provides information on majority ion equilibrium as well as on fluctuating velocities and temperatures [15]. It is apparent that all such studies cannot be undertaken simultaneously due to space limitations on the vacuum chamber ports and to other trade-off considerations or conditions that may make some of these impossible. Nevertheless, it is intended that CXRS and NPA will be fundamental for TJ-II while others such as BES may be undertaken at some future stage.

In order to justify the provision of a DI, several leading edge experiments could also be contemplated for the TJ-II. For instance, measuring the plasma poloidal flow inside static magnetic islands as performed in the Large Helical device (LHD) [16,17]. Also, the choice of DI type will also limit the type of experiments that can be carried out.

IV. Diagnostic Injector Types

In this section, several DI systems installed in, or planned for, other fusion machines are presented and an evaluation is made with regard to the suitability of such systems for the TJ-II stellarator. Then, several DI types that are available from the Budker Institute are presented and these are also evaluated.

IV.1 Diagnostic injectors in magnetically confined plasma devices

In the following subsections, brief reviews are given of the principal characteristics of DI neutral beams provided in some magnetically confined plasma devices that are similar in many respects to TJ-II.

i) *Madison Symmetric Torus*

Two compact DI systems are in operation in the Madison Symmetric Torus (MST) [18]. The first is a 20 keV, 4 A, helium beam optimised for Rutherford Scattering studies, while the second is a 30 keV, 4 A, hydrogen beam for CXRS and motional Stark effect (MSE) studies. In these injectors, ions are extracted from a plasma created by an arc discharge source and, after acceleration and focusing, neutralised in a gaseous target in the coupling between the ion source and main vacuum chamber. In addition, the low perpendicular temperature at the plasma emission surface results in a low (0.016 rad) beam divergence. This, together with the geometric focussing, provides a 5 cm diameter beam (1/e) with a quoted current density of ~400 mA cm^{-2} at the magnetic axis [17]. These ion sources are compact in size (30 cm in diameter and 70 cm length) and weight about 70 kg. However, the time duration of the pulse is limited to 3 ms by the power supply.

ii) *Textor*

The DI system developed for Textor [1] is larger and more complex than the system described above. The maximum beam energy available is 50 keV and, when operated with hydrogen, the ion source can provide up to 2 A of ion current with a pulse duration up to 4 s (the beam can be modulated with a frequency up to 500 Hz). Also, the typical current density is ~130 mA/cm^2 while the ion species composition is 71.5%, 13% and 15.5% for H^+, H_2^+ and H_3^+ respectively. In addition, the beam divergence is 0.5° to 0.6° and is geometrically focused 4 m downstream from the source to have a 1/e diameter of 70 mm at the focal point.

The ion source plasma is produced by a radio frequency discharge in hydrogen or helium, and the ion beam is extracted by a four-grid system with 163 single holes. In order to provide the long pulse a dedicated vacuum system is needed in order to avoid perturbating the vacuum in the main chamber. It comprises two liquid-helium cryogenic pumps, each with a pumping speed of 24000 l/s, and a turbo molecular pump with pumping speed of 250 l/s which is used for initial chamber pump down. As a result, this DI extends more than 5 m back from the main chamber, weighs several hundred kilograms, and can only be mounted horizontally. Similar systems have been developed for the Alcotor C-Mod [19] and for the TCV [20] tokamak devices.

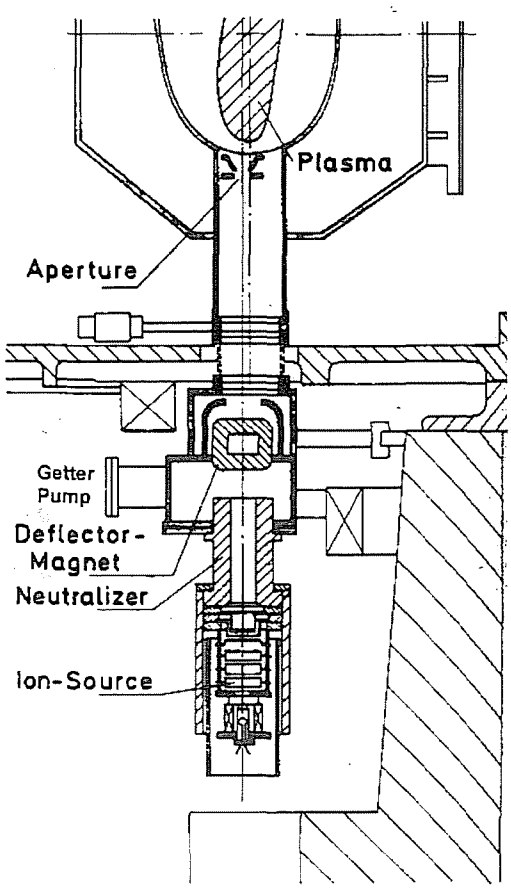

Figure 3. Cross-section through the W7-AS DI system. The beam is injected vertically upwards into the W7-AS main vacuum chamber.

iii) *Wendelstain 7-AS*

Figure 3 shows a cross-sectional view of the DI system used in the Wendelstein 7-AS (W7-AS) stellarator device [21]. The maximum beam energy available from this DI was 35 keV and when operated in hydrogen the source could deliver an ion current of up to 6 A for a pulse length of up to 400 ms. The composition of the ion species exiting this radio-frequency source was typically 90%, 7% and 3% for H^+, H_2^+ and H_3^+ respectively and the current density was $\leq$240 mA/cm^2 at the focus. The beam divergence was 1.4° (half divergence angle), and it was geometrically focused 2.1 m downstream from the source to create an effective diameter of ~10 cm, at the focal point (it was generally collimated down to 10 × 5 cm^2). In addition, the beam could be pulsed with an interval of $\geq$2 ms between pulses. Also, to provide the long pulse length a vacuum system comprising of 6 getter pumps, each with a pumping speed of 15000 l/s, and a turbo molecular pump, with 1000 l/s pumping speed, was needed. The system was mounted below the machine and the beam was injected vertically upwards into the plasma as shown in the figure. Note, that the neutralizer/ pumping chamber is not symmetric about its vertical axis, rather it is about 3 times wider in the plane perpendicular to the page in order to allow the large expansion volume required to fit into the space available below the W7-AS. Finally, this DI is now redundant as the W7-AS machine was shut down in 2002.

IV.2 Solutions offered by the Budker Institute of Nuclear Physics

In the summer of 2000, experts from the Budker Institute of Nuclear Physics in Novosibirsk visited CIEMAT and the TJ-II stellarator. During that visit, they offered three different types of diagnostic injector whose characteristics are reviewed in Table 1.

The first type (***Option-1***) proposed consists of a compact beam system with the advantages of a small beam diameter, ~3.2 cm, and relatively uncomplicated installation and manipulation. Also, its size and weight are reduced (~60 kg), while the vacuum, power supply and control system requirements are not excessive. For instance, the power supply and control system would occupy no more than two rack systems. Maintenance requirements are also expected to be minimum. However, it would appear that the principal drawback of this beam is its short pulse length, ≤5 ms, a value that could limit both neutral particle and spectroscopy unless its beam current density (200 mA/cm^2) can be increased (see Section V).

The second type (***Option-2***) proposed consists of a system similar to the RUDI injector installed on the Textor device [1]. Such a system would be both large and complicated, and would occupy a large volume of space, up to 4 m long, extending back from the injection port of the machine as well as considerable labour input and maintenance. Its main advantage is that pulse lengths up to 50 ms can be provided. However, this advantage is somewhat offset by the increased beam diameter, ~6cm, and a lower central current density, ≤120 mA/cm^2.

The third system (***Option-3***) offered by the Budker Institute is similar to the first but with the added advantage that two ≤5 ms pulses can be generated. However, the pulses must be separated by at least 100 ms in order to allow for vacuum system pump-out. This upgrade would require a second power supply system (which would double in size), as well as some modifications to the control system.

At a later time, and after some consultation with the Novosibirsk group, the possibility of renting an intermediate beam system was considered (***Option-4***). See Table 1. Although this ion source can provide pulses up to 50 ms long, the associated pumping system and available power supply would result in considerably shorter pulse lengths.

Subsequently, another possibility has also been considered. It is to choose a compact type system, with a short pulse length, but with increased current density [17] in order to increase signal levels (***Option-5***). The MST group at Madison has installed a similar system that includes a small, arc-discharge, ion source with a specially designed grid. The design results in a reduced perpendicular ion temperature at the plasma emission surface inside the ion source that gives reduced beam divergence and increased current density. Otherwise, the pumping systems *etc.* are similar to ***Options-1*** and ***-3***.

Lastly, while other suppliers have also been considered, for instance DANFYSIK A/S at Jyllinge, Denmark, they have proved to be unviable solutions.

IV.3 Alternatives

The possibility of using one of the TJ-II NBI heating beams [4] has also being contemplated. Some modelling has being performed in an attempt to identify a position were the heating beam intersects with the magnetic axis. The best positions correspond to the toroidal angle of 105° (sector A2 of Fig. 1), where good access could be achieved through the side and upper ports, and the toroidal angle of 120° (sector A4 of Fig. 1), where there no ports are currently available. The major drawback is that the beam diameter is almost equal to that of the plasma diameter, with the resultant lack of spatial resolution. Calculations have also been performed for the case where a collimator is placed in the beam close to its entrance to the TJ-II chamber. However, the result shows the resultant beam shape would be completely distorted at the two toroidal angles of interest and that the neutral current density would be reduced to a level that could not justify the approach.

IV.4 Conclusions

After reviewing all of these options, only two were considered viable for the TJ-II and for more detailed review. These were the ***Option-2*** and ***Option-5*** sources. Other options were considered not suitable either from scientific or engineering points-of-view. While the ***Option-5*** source is compact and can be mounted in any orientation, the ***Option-2*** type source is both large and complicated, requiring increased effort for building and maintaining, and can only be mounted horizontally, *i.e.* on the TJ-II platform floor. This is an important point, as it would require the NPA system (also large and complicated) to be mounted vertically either above or below the TJ-II. However, it offers a significantly longer pulse length with possible scientific gains to be obtained. These two options are reviewed in more detail in the following sections, in particular in terms of the requirements for performing neutral particle analysis and charge-exchange recombination spectroscopy.

	Option-1	Option-2	Option-3	Option-4 (Rent)	Option-5 (Madison-type)
Pulse length	≤5 ms	≤50 ms	≤5 ms	≤50 ms	≤5 ms
Modulation	1 pulse	Up to 200 Hz	2 single pulses #	-	2 single pulses†
Beam energy	10 – 40 keV	10 – 50 keV	10 – 40 keV	10 – 50 keV	10 – 30 keV
Extracted ion current	Up to 4 A	Up to 5 A	Up to 4 A	Up to 4 A	Up to 4 A
Divergence	<1°	0.7 °	<1°	0.7 °	<1°
*Focal length	1.3 m	2.2 – 2.5 m	1.3 m	1.5 m	1.245 m
Beam diameter at focus (1/e)	3.2 cm	4 cm	3.2 cm	4 cm	2.3 cm
Orientation	Arbitrary	Horizontal	Arbitrary	Horizontal	Arbitrary
Vacuum requirements	Turbo pump	Turbo 400 l/s + cryopump or Ti-getter	Turbo pump	Turbo pump	Turbo pump
Size	50 × 80 cm	1.5 × 2 m	50 × 80 cm	-	50 × 80 cm
Ion source weight	60 kg	500 kg	60 kg	-	60 kg
System control	Manual	Computer	Manual	-	Manual
Power supply size	$2 \times 2 \times .7$ m^3	$7 \times (.7 \times .7 \times 2)$ m^3	$2 \times 3 \times .7$ m^3	-	$2 \times 2 \times .7$ m^3
Delivery time	~1 year	~2 years	~1 year	~1 year	~1 year
TJ-II port requirement	A8 bottom, side or top	Large Side	A8 bottom, side or top	Large Side or A8 bottom	A8 bottom, side or top
NPA & CXRS Accessibility	Good	Problem for NPA	Good	-	Good
Estimated time for operation	2.5 years	5 years	2.5 years	2.5 years	2.5 years

Table 1. Summary of possible Diagnostic Injector systems for the TJ-II. Note that the cost of **Option-2** is approx 2.5 times that of **Option-5**. *The focal length given here is to aid comparison between systems. In TJ-II it is dependent on magnetic considerations. See Section VI. Time interval between pulses is ≥100 ms[#] and ≥50 ms[†].

V. Requirements for Neutral Particle Analysis and Charge Exchange Spectroscopy

V.1 Neutral Particle Analyser (NPA).

Neutral particle analysis has been employed to date in TJ-II to obtain majority ion temperature profiles. For this a neutral particle analyser system with two variable lines of sight though the plasma is installed [7]. It is equipped with two Acord-12 systems to measure the energy of neutral hydrogen particles that escape from the hot plasma [22]. These particles, which provide information about the majority ion temperature in the plasmas, are the product of charge exchange reactions involving a slow neutral H_s^0 and a fast central ion H_f^+,

$$H_s^0 + H_f^+ \rightarrow H_s^+ + H_f^0$$

The resultant fast neutrals H_f^0 can escape from the plasma without undergoing collisions to be detected by the NPA. However, the information obtained is not well localised as it involves the integration of reactions along the whole line-of-sight. To overcome this, a collimated neutral beam can be used to increase these reactions along a well-localised path. Hence, by comparing active and passive signals improved localised majority ion temperature profiles can be obtained.

Before determining the DI requirements, it should be noted that for passive neutral particle analysis the minimum signal integration time for TJ-II conditions is 2 ms. However, integration times between of 6 and 10 ms are normally required in order to improve statistics. Now to determine these requirements, simulations of NPA signals with and without a DI beam have been performed using the DOUBLE code [23]. This code simulates the plasma with representative electron density and temperature profiles. The code provides the DI and NPA with cylindrical coordinates that represent their locations in real space. It also takes account of the plasma to wall distance. Also, prior to executing the simulation some assumptions concerning the neutral density and temperature at the plasma edge are needed. Finally, from output of the code it is possible to compare active (A) and passive (P) signal levels.

For the TJ-II, calculations were performed for two ion temperature profiles with radial dependence $1\text{-}x^2$ and $1\text{-}x^4$, where x is effective radius. In Fig. 4, results of active/passive signal contrast, *i.e.*, (A+P)/P ratio, are presented. Note, when the DI is off, then A = 0 and (A+P)/P = 1. In contrast, when the DI is on, then signal contrast improves. For instance, if (A+P)/P = 1.2,

then the DI produces a 20% improvement in NPA signal. The ratio (A+P)/P is dependent on plasma parameters and, of course, on beam parameters. So in simulations, this ratio is estimated while modifying plasma parameters. It is thus found that the critical parameter is the neutral density at the plasma edge. This density can be decreased, for instance, by changing the location of the gas-puff valve, in order to reduce the passive signal. Another means of increasing the (A+P)/P ratio would be to increase the beam size but this would be done at the cost of reducing spatial resolution. Finally, there is the additional effect, *i.e.* the beam halo surrounding the beam, which can also can a reduction in spatial resolution. However, this is not included in the code.

Plasma minor radius (m)	0.17
Elongation	1.5
Neutral boundary density (m^{-3})	10^{16}
Ion density (m^{-3})	$1.6 \times 10^{19} \times (1-x^2)$
Electron temperature (eV)	$700 \times (1-x^2)^2$
Ion temperature (eV)	$200 \times (1-x^2)$
Beam energy, keV	10
Beam density (A/cm^2)	0.1
Beam width (m)	0.01

Table 2. DI beam and plasma (both hydrogen) values used in the DOUBLE code to simulate the active and passive NPA signals from the TJ-II. It is assumed that the NPA views the DI beam at 90°.

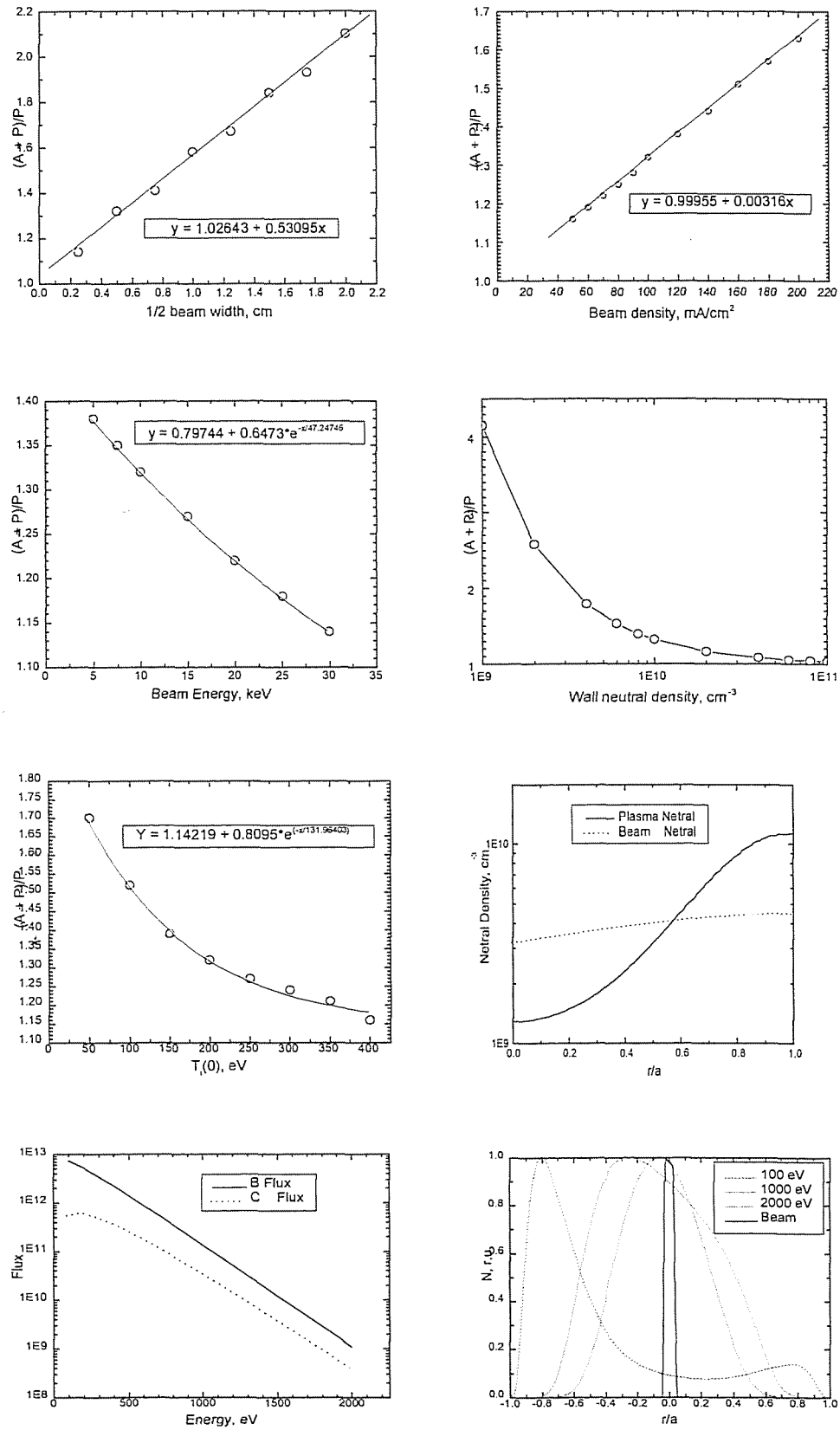

Figure 4. Dependence of contrast on a) beam half-width, b) beam density, c) beam energy, d) neutral density at plasma edge, e) ion temperature at plasma centre, and f) penetration of neutrals from the plasma edge to the centre. Also, g) the neutral flux leaving the plasma with (dashed) and without a DI (continuous line) and the f) normalised radial profile of neutrals with energies 100, 1000 and 2000 eV.

V.2 Requirements for Charge Exchange Recombination Spectroscopy

Charge exchange recombination spectroscopy involves the capture of the bound electron of a neutral hydrogen atom by a highly ionised ion into a highly excited state of the resultant ion with subsequent de-excitation by photon emission. The reaction of interest can be described by

$$H^0 + A^{+q} \rightarrow H^+ + A^{+(q-1)}(n,l) \rightarrow A^{+(q-1)}(n-1,1\pm1) + h\nu$$

where H^0 is the neutral hydrogen atom, A^{+q} and $A^{+(q-1)}$ are fully stripped and hydrogen-like ions, and n and l are the level and sublevel into which the transferred electron is captured. The excited hydrogen-like ion can subsequently de-excite via a cascade of $\Delta n = 1$ transitions involving the emission of photons with characteristic wavelengths. See Fig. 5. In the TJ-II, the main impurity ions include boron, carbon and oxygen [24], so the emissions from high upper levels occur in the ultraviolet-visible range while the photons emitted as a result of cascading tend to occur in the vacuum-ultraviolet range, a region that is more challenging from a spectroscopic point of view.

i) *Simulation of DI beam in TJ-II ECRH plasmas*

In order to evaluate the suitability of the DIs for performing active charge exchange recombination spectroscopy (CXRS) in TJ-II, it is necessary to determine the evolution of the beam size and its attenuation through TJ-II ECRH plasmas and estimate the resultant active spectroscopy signal levels. Note that for technical and scientific reasons only three of the DI outlined in Table 1 are considered here. See Table 4. It is also necessary to consider the collection and attenuation of the light signals in the optics as well as spectrometer and detector efficiencies.

When performing the simulation, it is first necessary to estimate the components of the beam that reach the TJ-II vacuum chamber, *i.e.*, the beam constituents after passing through the neutraliser. See Table 3. Then, from these, the beam equivalent current densities and the beam profile in the TJ-II vacuum chamber can be predicted using a model that was provided by the Swiss TCV group [20]. Note that beam losses due to interactions with the coupling and vacuum chamber entrance port are not considered here. Such losses become important if the TJ-II vacuum chamber access port is narrow. Next, by making some reasonable assumptions about the plasma, both the beam attenuation in the plasma and the beam current density

through the plasma can be determined. It is then possible to predict the emissivity of spectral lines from highly ionised species of impurity elements, *e.g.* carbon, again making some basic assumptions, based on collision rates between the beam neutrals and the completely ionised plasma impurities. Finally, the expected signal levels in a detector system attached to a spectrometer that receives light via fibre optic cables from the beam/plasma volume can be estimated. With these calculations, a judgement as to the suitability of an ion source for CXRS can be made.

	#Option-2	†Option-5
Ion source type	Radio frequency	Arc
Extracted ion current	≤5 A	≤4 A
Optimised beam energy (E)	10-50 keV	10 - 30 keV
Beam focal length	2.2 to 2.5 m*	Optional
Initial beam diameter	7 cm	8 cm
Beam divergence	~0.7°	~0.7°
Beam diameter at focus	40 mm	23 mm (~gaussian) for 1.3 m
Beam components (by current)	71.5% H^+; 13% H_2^+, 15.5% H_3^+	90% H^+; 5% H_2^+, 5% H_3^+
Disassociation of molecules in neutraliser	~100% for H_2^+ and H_3^+	100% for H_2^+ and H_3^+
Neutralisation efficiency for beam components (E, $E/2$, $E/3$).	0.50; 0.78; 0.85	0.72; 0.87; 0.88
Total Equivalent Current	4.778 equ. A	3.468 equ. A
Beam duration	≤50 ms	≤5 ms

Table 3. Parameters for three ion sources. #Values taken from Ref. [1]. †Values provided by the Budker Institute of Nuclear Sciences. *This length may need to be increased significantly because of space and magnetic considerations.

The extracted ion current in Table 3 refers to the total beam current exiting the ion source. As is apparent from the table, the beams have several components, (E, E/2 & E/3), with part of the beam current being lost during the neutralisation process. Hence, it is necessary to estimate the neutral flux exiting the neutralisation section of the system and the equivalent currents for the three energy components. For this, the exiting neutral flux for each energy component is obtained from the % ion beam component and neutralisation efficiency. See

Table 4 for these values for the ***Option-5*** source. Finally, the total equivalent current exiting the neutraliser is the summation of these contributions to the ion beam current.

Ion beam components	90% H^+	5% H_2^+	5% H_3^+
Neutralisation Efficiency	0.72	0.87	0.88
Neutral flux exiting neutraliser	0.9×0.72	$0.05 \times 0.87 \times 2$	$0.05 \times 0.88 \times 3$
Equivalent Current (equ. A)	2.592	0.348	0.528
Total Equivalent Current	3.468 equ. A		

Table 4. Estimates of the equivalent beam currents that exit the ***Option-5*** source. Note that disassociation is ~100% in the neutraliser and the extracted current is 4 A.

The extracted ion current in Table 3 refers to the total beam current exiting the ion source. As is apparent from the table, the beams have several components, (*E*, *E*/2 & *E*/3), with part of the beam current being lost during the neutralisation process. Hence, it is necessary to estimate the neutral flux exiting the neutralisation section of the system and the equivalent currents for the three energy components. For this, the exiting neutral flux for each energy component is obtained from the % ion beam component and neutralisation efficiency. See Table 4 for these values for the ***Option-5*** source. Finally, the total equivalent current exiting the neutraliser is the summation of these contributions to the ion beam current.

Next, knowing the equivalent current existing the neutralizer, a beam current density profile (in vacuum) can be created using equations (1) to (3) [20]. Here, $j(z,r)$ is the current density at a distance z from the ion source and at radius r from the beam centre. The equations are given by

$$j(z,r) = j(z,0)\exp\left(-\frac{\pi}{I} j(z,0) r^2\right) \qquad (1),$$

$$j(z,0) = \frac{I}{\pi a^2}\frac{z^{*2}}{z^2}\left(1 - \frac{a^2}{z^{*2}\tan^2\varphi}\right) \qquad (2),$$

$$\frac{1}{z^*} = \frac{1}{z} - \frac{1}{z_{foc}} \qquad (3),$$

where a and φ are the ion source radius and the beam divergence respectively, and z_{foc} is the source exit to plasma centre distance. After taking magnetic considerations in account (the

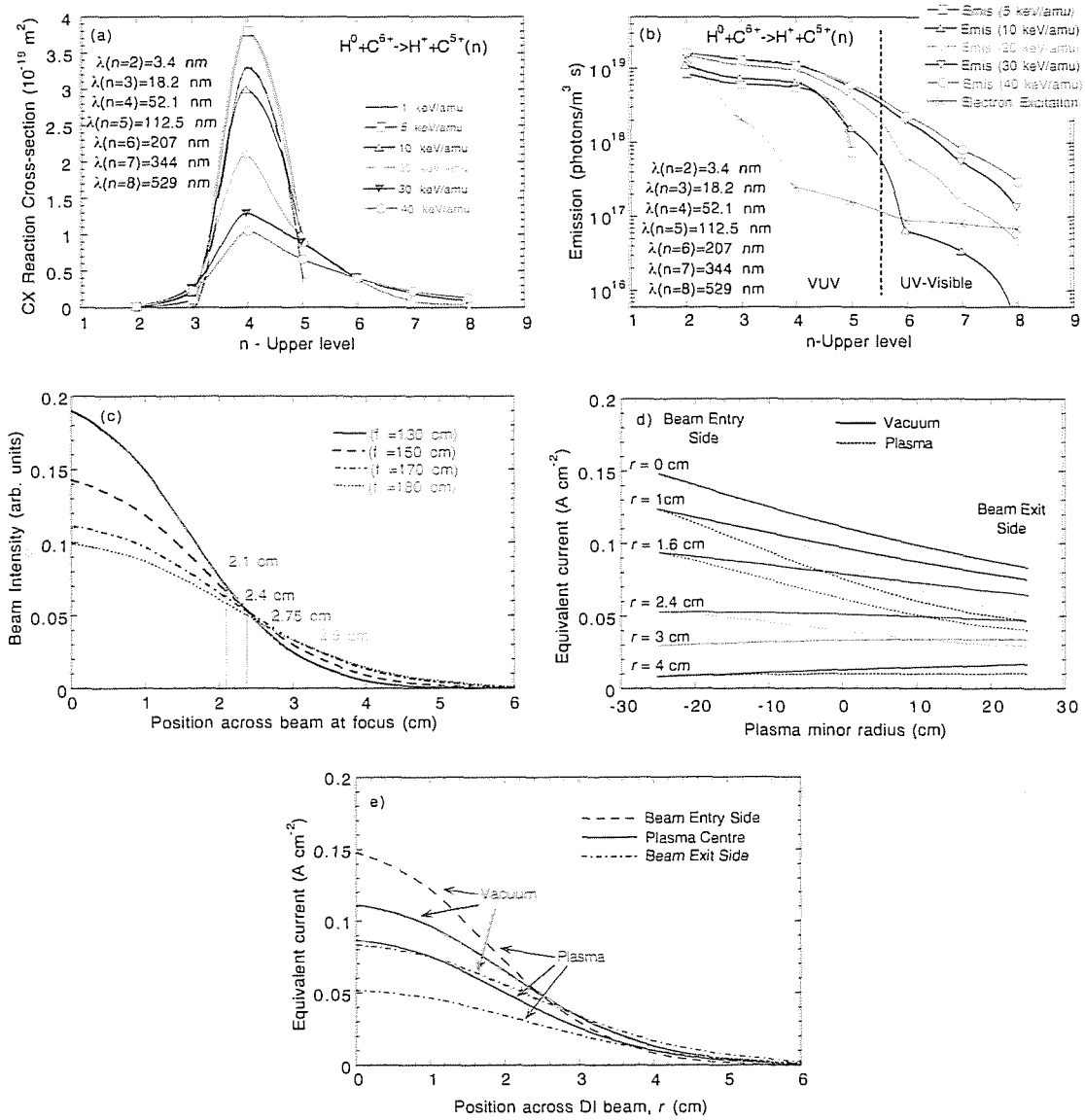

Figure 5. a) Partial electron capture cross-sections for charge exchange between neutral hydrogen (1 to 40 keV/amu) and fully stripped carbon ions, $H^0 + C^{+6} \rightarrow H^+ + C^{+5}$ (n). b) Emission rate cross-sections for charge exchange (***Option –5*** DI) and electron excitation c) DI neutral beam profiles (*E* component), at beam focus, for several DI focal lengths. The values shown represent the radii for1/e intensity. d) DI neutral beam fall-off about plasma centre (*E* component) for vacuum and ($\tilde{n}_e = 1.2 \times 10^{19}$ m^{-3}) plasma conditions with z_{foc} = 1.7 m. e) Variation in the neutral beam profile for same vacuum and plasma conditions.

source is shielded with ferromagnetic material) z_{foc} is set to 170 cm. See section VI.3. Now applying these equation for TJ-II the beam equivalent current across the minor radius for vacuum conditions are determined and plotted in Fig. 5. These equations are for vacuum conditions so it is now necessary to consider the beam attenuation in representative plasmas. For this, it is assumed that TJ-II plasmas can be approximated with a single impurity (charge number *Z*). For this the standard equation for beam attenuation can be applied. It is given by

$$I(z) = I(z_0)\exp\left(-\int_{z_0}^{z} \lambda dz\right) \qquad (4),$$

$$\lambda = n_e\left(\frac{\langle\sigma_e v_e\rangle}{v_b} + \frac{Z - Z_{eff}}{Z-1}\sigma_{totH} + \frac{Z_{eff}-1}{Z(Z-1)}\sigma_{totZ}\right) \qquad (5).$$

Here, σ_e is the impact cross-section for electrons while σ_{totH} and σ_{totZ} represent the H^0 impact total cross-sections (charge exchange and ionisation) for protons and ions. Next Z_{eff}= 2 is assumed for TJ-II and carbon is selected as a representative ion, *i.e.* Z = 6. As this modelling is quite involved and time consuming, the beam attenuation for a 50 keV beam in a TCV plasma with $T_e(0)$ = 1.2 keV and $\tilde{n}_e(0)$ = 1.4×10^{19} m^{-3} was adapted to the TJ-II. These values represent the maximum electron and temperature values for standard ECRH plasmas in TJ-II. Applying these to the previous results for vacuum conditions, the beam attenuation as well as the beam current density and beam width at focus can be estimated. See Fig. 5.

ii) *Simulation of CXRE ion temperature measurements*

Now having modelled the beam attenuation in the plasma, the emissivity of spectral lines from highly ionised ions (*e.g.* C VI) can be estimated. For this, some knowledge of the charge exchange reaction cross-sections and the local ion and beam densities is needed. The equation used to estimate emissivity is

$$E = \frac{\eta_Z \eta_{H^0}\langle\sigma v\rangle_{CX}}{4\pi} \qquad \text{photons m}^{-3}\text{ sr}^{-1}\text{ s}^{-1} \qquad (6),$$

where η_{H0} is the local neutral beam current density, η_z is the local C VII (fully stripped) ion density, and $\langle\sigma v\rangle_{cx}$ is the charge exchange rate-coefficient for excitation of wavelength λ for 30 keV H^O neutrals impacting on fully stripped ions. Hence, the averaged emissivity of the C VI spectral line at 529 nm excited by the ***Option-5*** beam is estimated from Eq. (6) to be

$$E = (5 \times 10^{16}\text{ m}^{-3} \times 6.87 \times 10^{14}\text{ m}^{-3} \times 4.8 \times 10^{-15}\text{ m}^3\text{ s}^{-1})/(4 \times \pi)$$

which gives

$$E = 1.32 \times 10^{16}\text{ photons m}^{-3}\text{ s}^{-1}\text{ sr}^{-1}.$$

The estimated emissivity excited by the ***Option-2*** beam under the same conditions is E = 5.1 $\times 10^{15}$ photons m^{-3} s^{-1} sr^{-1}.

Next, it is necessary to consider the observation chord length, l, the viewing geometry entendue, G, the optics, spectrometer and detector efficiency, k, and the beam duration, t_{pulse}, and to include a weighting factor to account for the average beam current density along the view chord, w, in order to determine the photons detected by the photon detector, T. For this

$$T = k \cdot l \cdot w \cdot E \cdot G \cdot t_{pulse} \quad \text{counts} \qquad (7),$$

where

$$G = S_{image} S_{lens} / d^2 \quad \text{m}^2\ \text{sr} \qquad (8).$$

Here, l is determined by the total DI beam diameter at focus, *i.e.*, l ~0.112 m and w = 4.8 for ***Option-5*** (as determined by integrating the neutral current along the viewing chord). The terms in G are the DI beam to collecting lens separation, $d \approx 0.75$ m, the area of the DI beam being observed, $S_{image} = 7.8 \times 10^{-5}$ m^2 for 1 cm resolution, and the collecting optics surface area, $S_{lens} = 4 \times 10^{-5}$ m^2. Here, S_{lens} is determined by the fibre-optic core diameter, say 600 mm, and by the numerical aperture of the spectrometer, *i.e.*, N.A. = 0.06 for a 1 m Czerny-Turner. For these conditions, $G = 5.55 \times 10^{-9}$ m^2 sr. The spectrometer system efficiency, k of Eq. (7), is determined by the transmission of the fibre optics (T_{fo} ~98 % for 5 m of fibre), the transmission and reflectance of the window and lens (T_o ~79% at 529 nm), and by the efficiency of the spectrometer, *e.g.*, by the reflectivity of the 5 reflecting surfaces in a Czerny-Turner type (0.9^5 at 529 nm), the grating (~10%), and the CCD (~60% for a modern back-illuminated device). Hence, for a conceptual system, k = 0.027. The results of these estimates are given in Table 5.

Diagnostic Injector	***Option-2***	***Option-5***
Average Beam Current Density (A m^{-2})	70.2	263.9
Beam Averaged Emissivity (photons s^{-1} m^{-3} sr^{-1})	3.5×10^{15}	1.31×10^{16}
Pulse length (s)	0.05	0.003
Average Beam Current along View Chord (A m^{-2})	140.1	482.9
Weighting Factor, w	1.99	1.83
View Chord Length (m)	0.18	0.112
Photons collected per pulse	10^4 counts	1.2×10^3 counts

Table 5. Summary of the estimates of the C VI (λ =592 nm) CXRS photons detected with the ***Option-2*** and ***Option-5*** Diagnostic Injector systems.

iii) *Ion temperature measurements*

Now, for a 1200 lines/mm grating (dispersion = 0.833 nm/mm), a 20 μm pixel CCD, and an instrumental full-width at half-maximum (*FWHM*) of 0.072 nm [25], the 529 nm

emissions from 100 eV C VI ions would result in a measured line FWHM of 0.138 nm, or ~8 CCD pixels. Assuming Zeeman and Stark effects to be negligible, it then is estimated that the ion temperature could be determined within a 1σ uncertainty of ~23 eV for 1 cm resolution at the plasma centre. For measurement with reduced spatial resolution (2 cm), the 1σ uncertainty would reduce to ~11 eV. These cases are for ECRH plasmas with $n_e(0) = 1.3 \times 10^{19}$ m^{-3}. For NBI heated plasmas, where the DI beam attenuation is 3 to 4 times higher, the 1σ error would be $\Delta T_i = 50$ eV for 1 cm resolution and $\Delta Ti = 23$ eV for 2 cm resolution. See Fig. 5. Note that for NBI heating, the increased ion temperature will cause the relative error $\Delta T_i/T_i$ to decrease. The 1σ level can be reduced for NBI heating by increasing the DI pulse length to 50 ms, *i.e*, $\Delta T_i = 10$ eV for 1 cm or $\Delta T_i = 5$ eV for 2 cm resolution.

iv) *Ion velocity measurements*

In a previous work based on the 227.7 nm emission line from He-like carbon, *i.e.* C V, localised ion poloidal velocities of the order 2 km s^{-1} were measured [26]. Now, assuming that the C VI ion velocity is of the same magnitude, the shift in the 529 nm emission line due to poloidal rotation would be ~0.0035 nm. This shift, which is equivalent to 1/40 of its predicted Doppler *FWHM* (0.138 nm), is similar to the measured line-shift detection limit for lines with 1.5×10^3 counts, *i.e.* ~0.0038 nm. Note that this limit does not reduce linearly with counts, rather it is more effective to increase spectral resolution or line shift. Now, by using a 2400 lines/mm grating this uncertainty can be reduced. Moreover, this uncertainty could be further reduced more by viewing the DI beam from both red and blue shift directions, thereby doubling the relative shift. Unfortunately, the vertical beam DI in sector A8 does not permit this, so an alternative beam orientation would be required, *e.g.* horizontal beam injection in sector A8 is considered in Section VI. In conclusion, the choice of DI is not critical for measuring ion rotation once a high-resolution spectroscopic system is employed and if red and blue shifts can be measured simultaneously.

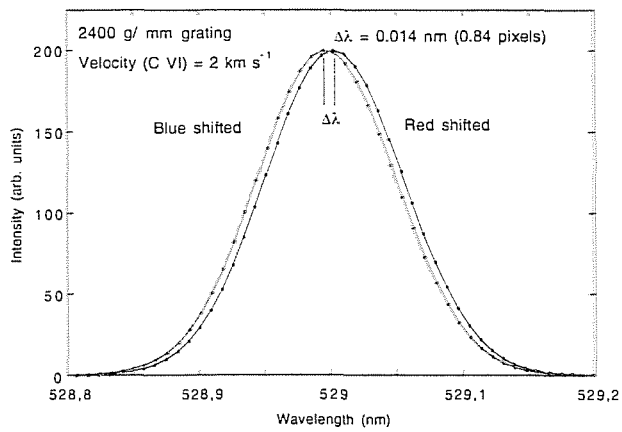

Figure 6. Simulation of idealised blue and red shifted C VI lines (at 592.1 nm) to determine relative shift for the TJ-II plasma rotating at 2 km s^{-1}. For this a 2400 lines mm^{-1} grating was assumed.

VI. Ion source location, beam orientation and other considerations

In addition to the DI type, several other important considerations need to be addressed. These include the DI location, its distance from the plasma centre and its orientation. As previously outlined in Section II, there exist a limited number of suitable access ports. After reviewing these the top and sides ports of Sector A8 have been identified to be most suitable. However, it is still necessary to determine the optimum neutral beam orientation, *i.e.* vertical or horizontal, as a trade off between spatial resolution, beam shine-through, and the ease of access for the detection systems. Furthermore, the perturbation of the ferromagnetic shielding that surrounds the ion source on the magnetic configuration needs to be considered in order to estimate the beam focal length. Finally, the beam injection angle must also be optimised in order to minimise particle trapping. Note that in the TJ-II there is significant variation in access port size and width so in some cases access port size can limit this angle.

VI.1 The ion beam orientation

Two ion source orientations have been considered. The first, as outlined above, is a vertical beam through the plasma with the ion source on top of the TJ-II. The second is to install the beam source so as to provide a horizontal beam through the plasma and place the diagnostic devices above or below the TJ-II. The principal benefits of such action would be a significant increase in the spatial resolution along the beam direction (or about 60% increase in the signal levels while maintaining the same spatial resolution at in the vertical beam case) and provide better relative localisation of the beam along the line of sight. Note, at port location A8, a doubling of resolution, or of signal levels, is based on the simple assumption that the horizontal beam path through the plasma is about half that of the vertical beam path through the plasma, so that the beam intensity is considerably higher for the horizontal case. However, an important consideration is beam shine-through onto the hardcore with the possible consequences being sputtering of iron into the plasma and the creation of a localised halo (downward and upward looking chords- improved velocity measurements – should help to identify blue and red shifts).

VI.2 Neutral beam sputtering and reflection off the hardcore

In order to determine the magnitude of sputtering and the reflected beam we consider a worst-case scenario, *i.e.* a 20 keV beam (2.7 equ. A, area ~20 cm^2 at the 1/e level) with close to 100% beam shine-through. In the case of sputtering, Eckstein *et al.* [26] provide curves of the sputtering yield for H^0 atoms incident on iron. For 20 keV H^0, the quoted sputtering yield

is ~6 $\times 10^{-3}$ iron atoms per incident hydrogen atom. Hence, for a 3 ms duration pulse, approximately 2.4×10^{16} H^0 atoms will reach the hardcore and sputter ~1.5×10^{14} iron atoms. Now, assuming that these iron atoms penetrate into the plasmas to become ionised, then for a $T_e(0)$ = 1 keV plasma, the iron can loose up to 16 electrons per atom to the plasma, or ~2.3×10^{15} electrons in total. This is equivalent to a perturbation of less than 0.001 % in electron density. The expected increase in plasma impurity content will also be minimal, as 1.5×10^{14} iron atoms represent about 0.001% the number of iron atoms injected into the plasma by the laser ablation technique. Finally, the particle, energy and mean energy coefficients for the conditions above are $R_N = 3 \times 10^{-3}$, $R_E = 7 \times 10^{-4}$, and $R_N/R_E = 0.2$ respectively. As the neutral beam current produces ~1.7×10^{19} H^0 particles incident on a ~20 cm^2 surface, the particle flux reflected back into the plasma will be ~2.5×10^{15} $H^0\,cm^{-2}\,s^{-1}$ with mean energy ~4keV. When compared to the particle recycling rate, ~10^{17} $H^0\,cm^{-2}\,s^{-1}$, this represents an increase of a few percent. Finally, the equivalent current of the 4 keV reflected beam will ~10 mA, (in reality this beam will be well dispersed), a value that is not expected to perturb charge exchange measurements.

VI.3. The ferromagnetic shield surrounding the ion beam source

The ion sources offered by Novosibirsk are surrounded by a thin, high magnetic permeability, screen. The effect of such material has to be taken into account as it can give rise to a perturbation of the TJ-II magnetic configuration. In tokamaks such effects may be of secondary consideration and such sources can be located quite close to the plasma [18]. However, in stellarators the magnetic configuration is much more sensitive and considerable care is required to minimise perturbations. In order to evaluate the influence of this shielding, in particular for the compact source, and at the same time, determine the ion source to plasma centre separation necessary to minimise such perturbations, a study of the magnetic field effect has been performed.

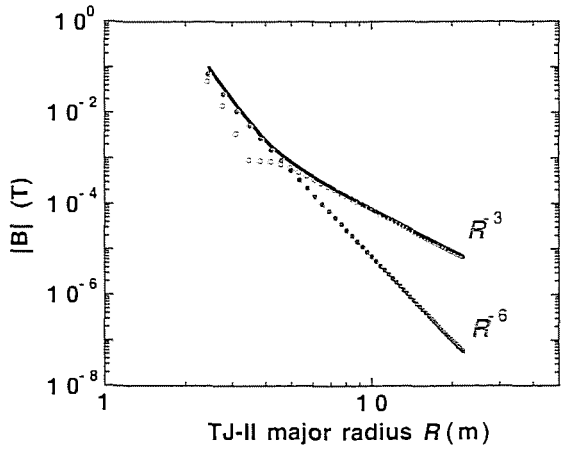

Figure 7. Plot of |**B**| as a function of cylindrical major radius. Plotted in red are the central (CC) and vertical field (VF) coils and in blue the toroidal field (TF) coils.

First, the TJ-II heliac produces a stray field around it whose typical radial dependence is shown in Figure 7. The toroidal field (TF) coils produce a high-order multi-polar field with an R^{-6} dependence, where R is the radial distance from the TJ-II centre [2]. The other coils, the central coil (CC), the helical field coil (HX), and the vertical field coil (VF) produce a dipolar field with an R^{-3} dependence. For large distances from the machine, the dipole component of the source is the significant one, and an effective dipolar moment can be defined to characterize the stray fields. With this field dependence, the influence of the TJ-II field on nearby magnetic materials can be reduced to an acceptable level by simply increasing the separation between the material and the TJ-II. Otherwise, if the materials react with the magnetizing field in a linear or similar way, *i.e.*, if they do not exhibit saturation or hysteresis, then the magnetization behaves in accordance with the same power laws while the back-effect on the magnetic configuration behaves as the distance from the TJ-II raised to a higher exponent.

A protocol was defined for this kind of magnetic materials. Soft ferromagnetic materials, such as those used for shielding, behave like permanent magnets. Their effect on the TJ-II magnetic configuration can be determined by considering a set of magnetic dipoles that approximate the far-field of the ferromagnets. In the case of a hollow cylinder, a model that considers the cylinder as several circular coils can give a good first estimation. Then a comparison of the calculations for each of these coils provides a first estimation of the influence of these materials on the TJ-II plasma configuration.

As it is considered that the most harmful influence of field errors on the TJ-II is the onset of large magnetic islands at rational values of $\iota/2\pi$, two vacuum configurations have been selected. These are the **100_36_61** and **100_40_63** configurations[1], which are similar in shape and plasma volume [28, 29]. The lowest order $\iota/2\pi$ rational values are 3/2 (non-natural value) for **100_36_61** and 8/5 (natural value) for **100_40_63.**

---

[1] The TJ-II flexible heliac has a wide range of magnetic configurations that can be accessed by varying the currents in its external coils. There are four coils whose currents can be varied independently; these are I_{CC}, the central circular coil current, I_{HX}, the helical coil current, I_{TF}, the toroidal field coils current, which are fed in series, and I_{VF}, the vertical field coil current. However, during plasma operation with ECRH, the condition of electron cyclotron resonance for $|B|$ restricts the independence of these four current sets. For this I_{TF} is determined once the remaining currents have been defined, while the current set (I_{CC}, I_{HX}, I_{VF}) defines the TJ-II configuration. Moreover, the three numbers that define the configuration are the integer values closest to these currents (in kA) multiplied by 10, *i.e.* in the order CC_HX_VF. For example, the configuration with currents I_{CC} = 9.98 kA, I_{HX} = 3.19 kA, I_{VF} = 5.99 kA, and I_{TF} = 27.28 kA is labelled 100_32_60.

Now in order to simplify the task, the soft ferromagnetic screen about the ion source has been modelled as a spherical shell of infinite permeability. For this case, the magnetic dipole moment of the shell, m, in a uniform magnetic field, B_0, can be given by [30],

$$m = 4\pi / \mu_0 \times B_0 \times b^3 \quad \text{(SI units)} \qquad (9),$$

where b is the outer radius of the spherical shell. In reality, some adjustments to this expression may be needed because of field gradients, the finite value of the magnetic permeability and the real geometry of the ferromagnetic material. Nonetheless, when setting b = 0.3 m, $\mu_r = 10^4$ and a screen thickness of 0.01 m, the estimated error is less than 0.2%.

However, in reality it is very difficult to simulate the real TJ-II B-field and the true geometry of the screening material. For this reason, the approximation made is to calculate the magnetic field produced by the TJ-II coils at the centre of the shield. For this a circular coil with a magnetic dipole close to that estimated for the spherical shell has been used. The modified magnetic surfaces as well as the iota and magnetic well profiles for the two configurations selected have been calculated. Note that the orientation of this coil does not influence the result.

Figure 8 shows the resultant transform and well profiles for four cases. The first is for an ion source with no screening material, while the following three are for increasing distances between the ion source focussing grid and the mid-plane of the TJ-II. The distances selected for this were 1.0, 1.4, and 1.7 m. Larger separations were not considered for the compact DI as at such distances the beam diameter and current density at the plasma centre become unacceptable for performing physics. Now, it is apparent from Fig. 8 that the magnetic shield has a minor influence on the rotational transform and magnetic well profiles. It can be concluded that only rational transforms already present in the configuration need to be considered and that no significant impact on Magnetohydrodynamic (MHD) stability, which is dependent on magnetic well, is to be expected.

Finally, the modelling has shown that the influence of shielding on magnetic islands, which arise at low order rational values of iota, ι, can be significant.[2] For instance, natural

---

[2] In a torus, a magnetic field line, when followed the long way around, will either close upon itself after a finite number of transits n or continue indefinitely to ergodically cover a surface or volume [31]. Field lines that close upon themselves lie on toroidal magnetic surfaces, called rational magnetic surfaces. Magnetic islands can arise in magnetic traps close to these rational magnetic surfaces. These surfaces are defined by the rotational transformation angle, iota, $\iota = n/m$ (where n and m are integers). In this case, the perturbating magnetic field contains harmonics of the form $\cos(n\varphi - m\theta)$, where φ and θ are the angle variables along the major and minor

islands, *i.e.* $\iota/2\pi$ = n/m, such as the 8/5 in the **100_40_63** configuration are barely affected, see Fig. 9, but low-order non-natural islands, such as the 3/2 in the **100_36_61** configuration, can be strongly influenced by the shielding material. See Fig. 10. Hence, it is only at the large separation, where the residual TJ-II field is ≤0.01 T, that such magnetic islands are similar in size to those occurring when no ion source is present.

VI.4. A solution to minimize perturbations due to magnetic shielding

As outlined above, it is undesirable that the DI ion source shielding should cause perturbations to TJ-II magnetic configurations. On the other-hand, the DI should be located as close as possible to the plasma centre in order to optimise measurement localisation. A possible compromise is to mount the DI on a translatable system so that it can be withdrawn to a suitable distance when not in use or when sensitive magnetic configurations are present. Such a system might consist of the compact DI mounted on a translation coupling that consists of an extendable/compressible vacuum bellows and support system. Furthermore, since the DI focal length is fixed and since the plasma location varies with magnetic configuration, such a system would permit adjustment of the neutral beam focal position in accordance with experimental needs. In such case, a DI focal length of 1.x m would be acceptable.

VI.5. The beam injection angle

In order to avoid creating trapped particles, the beam should not enter the plasma perpendicular to its plasma surface. However, this will not be a problem in the TJ-II as a vertical or horizontal neutral beam will enter the plasma at an angle of ~20° to the plasma surface normal. The possibility of increasing radial resolution by injecting the beam through the shortest distance (magnetic surfaces closer) is considered.

---

circumferences of the torus. The magnetic islands twist their way around the plasma and have their own set of nested flux surfaces and local magnetic axis. The whole structure of each island closes upon itself after continuing around the torus one or more times. Each island can further subdivide into smaller islands, and the smaller islands into finer islands, and so on.

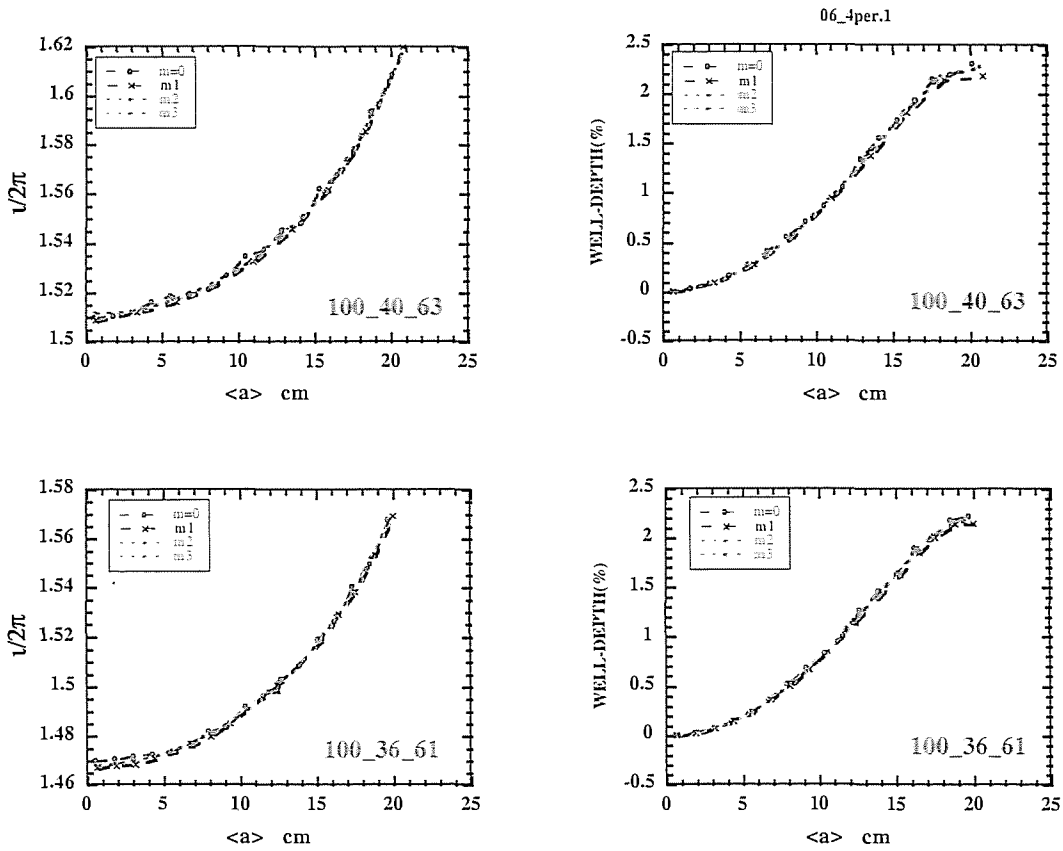

Figure 8. Rotational transform and magnetic well plasma profiles, across the plasma minor radius $<a>$, for the configurations **100_40_63** and **100_36_61**, and for several DI ion source (focussing grids) to plasma centre distances. These are 1.0 m (***m1*** = 27×10^3 A m^2), 1.4 m (***m2*** = 5.4×10^3 A m^2), 1.7m (***m3*** = 2.7×10^3 A m^2) and infinity (no screening material). Here, ***m*** is the magnetic dipole moment.

VII. Conclusion

After careful considerations from scientific, engineering and technical points of view, it was decided to opt for an ***Option-5*** type diagnostic injector, the DINA-5F, with a focusing ion optical system consisting of four multi-aperture spherically curved electrodes [18]. The principal parameters of the system selected are outlined in Table 6. It is envisaged that this system will be mounted in sector-A8 of the TJ-II with the beam injected from the side port as shown in Fig. 2b in order to optimise both NPA and CXRS data collection.

Beam Energy	15 – 30 keV
Extracted ion current	4 A
Individual pulse duration	≤5 ms
Number of pulses in chain	2
Minimum interval between pulses in chain	50 ms
Proton fraction	> 80%
Injector weight	~60 kg
Focal distance	To be specified

Table 6. Summary of the parameters for the neutral beam injector selected for TJ-II.

Acknowledgements

This work was partially funded by the Spanish *Ministerio de Ciencia y Tecnología* under Project FTN2000-0933. We are also indebted to Drs. E. Ascasíbar, C. Hidalgo, and J. Sánchez for their helpful discussions and also to Drs. J. Guasp, M. Liniers, F. Tabarés and C. Fuentes for their advice. The support of the TJ-II team is also acknowledged.

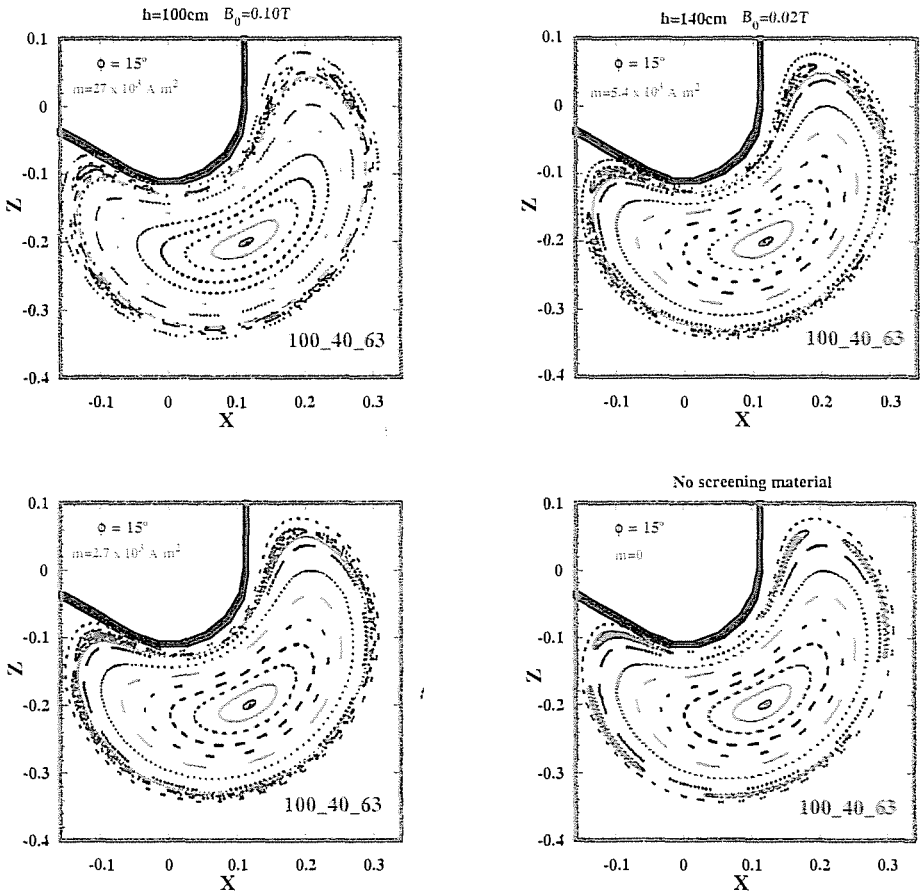

Figure 9. Flux surfaces for the 100_40_63 magnetic configuration which include the $i/2\pi$ = 8/5 rational value. The four $\boldsymbol{m}$ (magnetic dipole) values considered in Fig. 8 are shown. These are a) 1.0 m ($\boldsymbol{m} = 27 \times 10^3$ A m^2), b) 1.4 m ($\boldsymbol{m} = 5.4 \times 10^3$ A m^2), c) 1.7m ($\boldsymbol{m} = 2.7 \times 10^3$ A m^2) and d) infinity (no screening material).

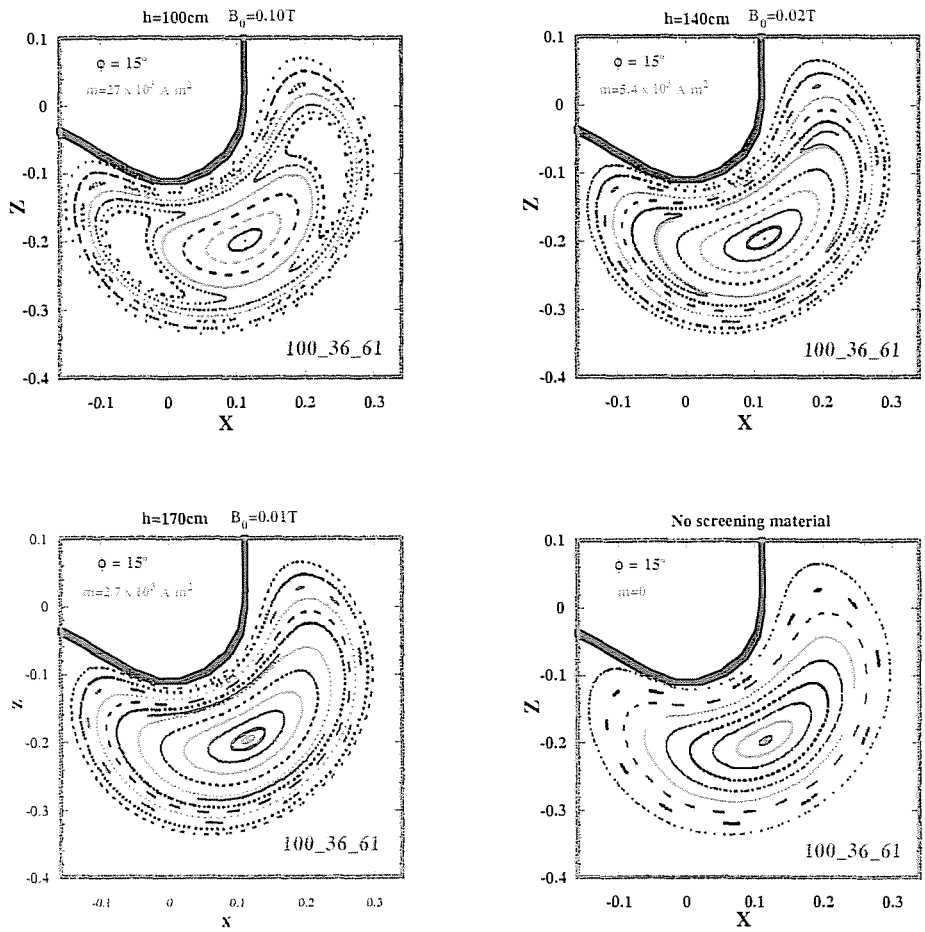

Figure 10. Flux surfaces for the **100_36_61** configuration which contains the $\iota/2\pi = 3/2$ rational value. The four $\boldsymbol{m}$ (magnetic dipole) values considered in Fig. 8 are shown. These are a) 1.0 m ($\boldsymbol{m} = 27 \times 10^3$ A m^2), b) 1.4 m ($\boldsymbol{m} = 5.4 \times 10^3$ A m^2), c) 1.7m ($\boldsymbol{m} = 2.7 \times 10^3$ A m^2) and d) infinity (no screening material).

References

[1] A. A. Ivanov, V. I. Davydenko, P. P. Deichuli, A Kreter, V. V. Mishagin, A. A. Podminogin, I. V. Shikhovtsev, B. Schweer, and R. Uhlemann, Rev. Sci. Instrum. 71 (2000) 3728.

[2] E. Ascasíbar *et al.* Fusion Eng. Des. 56-57 (2001) 145.

[3] C. Alejaldre *et al.*, Plasma Phys. Control. Fusion 41 (1999) A539.

[4] J. Guasp, M. Liniers, C. Fuentes, and G. Barrera, Fusion Technol. 35 (1999) 32.

[5] IPP Annual Report (1992), Max-Planck-Institut Fur Plasmaphysik, Garching Bei Munchen, Germany.

[6] J. Sánchez *et al.*, J. Plasma Fusion Res. SERIES, 1 (1998) 338.

[7] J. M. Fontdecaba, R. Balbín, S. Petrov, and TJ-II team, CIEMAT Report 1014 (February 2003).

[8] F. M. Levinton, Rev. Sci. Instrum. 70 (1999) 810.

[9] E. S. Marmar J. L. Terry, W. L. Rowan, and A. J. Wootton, Rev. Sci. Instrum. 68 (1997) 265.

[10] W. L. Rowan, R. V. Bravenec, E. C. Eisner, D. W. Ross, A. J. Wootton, N. Bretz, E. S. Marmar, and J. L. Terry, Rev. Sci. Instrum. 70 (1999) 882.

[11] G. McKee, R. Ashley, R. Durst, R. Fonck, M. Jakubowski, K. Tritz, K. Burrell, C. Greenfield, and J. Robinson, Rev. Sci. Instrum. (1999) 913.

[12] W. Mandl, R. C. Wolf, M. G. von Hellermann, and H. P. Summers, Plasma Phys. Control. Fusion35 (1993) 1373.

[13] R. C. Isler, Plasma Phys. Control. Fusion, 36 (1994) 171.

[14] J. C. Reardon, D. Craig, D. J. Den Hartog, G. Fiksel, and S. C. Prager, Rev. Sci. Instrum. 74 (2003)1892.

[15] J. C. Reardon, G. Fiksel, C. B. Forest, A. F. Abdrashitov, V. I. Davydenko, A. A. Inanov, S. A. Korepanov, S. V. Murachtin, And G. I. Shulzhenko, Rev. Sci. Instrum. 72 (2001) 598.

[16] K. Ida, T, Morisaki, Y. Nagayama, S. Inagaki, K. Itoh, Y. Liang, K. Narihara, A. Yu. Kostrioukov, B. J. Peterson, K. Tanaka, T. Tokuzawa, K. Kawahata, H. Suzuki, A. Komori, and LHD Experimetal Group, Phys. Rev. Lett. 88 (2002) 1.

[17] K. Ida, S. Kado, and Y. Liang, Rev. Sci. Instrum. 71 (2000) 2360.

[18] G. F. Abdrashitov, V. I. Davydenko, P. P. Deichuli, D.J. Den Hartog, G. Fiksel, A. A. Ivanov, S.A. Korepanov, S. V. Murakhtin, and G. I. Shulzhenko, Rev. Sci. Instrum. 72 (2001) 34.

[19] W. L. Rowan, R. D. Bengtson, R. V. Bravenec, H. He, J. Jagger, D. M. Patterson, D. W. Ross, P. M. Valanju, A. J. Wootton, E. S. Marmar, J. H. Irby, J. A. Snipes, and J. L. Terry, Rev. Sci. Instrum 68 (1997) 300.

[20] J. Mlynar, "*TCV DNBI Profile and Attenuation Studies with Code Manual*", Report LRP 692/01, CRPP EPFL, Lausanne 2001.

[21] J. Baldzuhn, W. Ohlendorf and W7-AS-Team, Rev. Sci. Instrum. 68 (1997) 1020.

[22] A.B. Izvozchikov, M.P. Petrov, S. Ya. Petrov, F.V. Chernyshev and I.V. Shustov, Sov. Phys. Tech. Phys. 37 (1992) 201.

[23] Yu. N. Dnesrovskij, S. E. Lysenko and A. I. Kislyakov, Nucl. Fusion 19 (1979) 293.

[24] K. J. McCarthy, B. Zurro, and A. Baciero, CIEMAT Report 988 (March 2002).

[25] K. J. McCarthy, B. Zurro, and A. Baciero, CIEMAT Report 965 (May 2001).

[26] A. Baciero, B. Zurro, K. J. McCarthy, C. Burgos, and V. Tribaldos, Rev. Sci. Instrum. 72 (2001) 971.

[27] W. Eckstein, C. García-Rosales, J. Rooth, and W. Ottenberger, "*Sputtering Data*", IPP Report 9/82 (1993).

[28] T. C. Hender, J. L. Cartrell, J. H. Harris, B. A. Carreras, V. E. Lynch, J. F. Lyon, J. A. Fabregas, J. Guasp, A. López-Fraguas, and A. P. Navarro, Fusion Tech. 13 (1988) 521.
[29] E. Ascasíbar, Q. Jiang, and A. López-Fraguas, J. Plasma Fusion Res. 1 (1998) 183.
[30] J. D. Jackson "*Classical Electrodynamics*", John Wiley & Sons, (1975).
[31] A. I. Morozov and L. S. Solov'ev in: "*Reviews of Plasma Physics Volume 2*" Edited by M. A. Leontovich, Consultants Bureau, New York (1966).